THE KUIPER BELT AND ITS PRIMORDIAL SCULPTING

A. MORBIDELLI
Observatoire de la Côte d'Azur, Nice, France
(E-mail: morby@obs-nice.fr)

M.E. BROWN
California Institute of Technology, Pasadena, California

H.F. LEVISON
SWRI, Boulder, Colorado

Observatoire de la Côte d'Azur, Nice, France

Abstract. We discuss the structure of the Kuiper belt as it can be inferred from the first decade of observations. In particular, we focus on its most intriguing properties – the mass deficit, inclination distribution, the apparent existence of an outer edge and of a correlation among inclinations, colours and sizes – which clearly show that the belt has lost its pristine structure of a dynamically cold proto-planetary disk. Understanding how the Kuiper belt acquired its present structure will provide insight into the formation of the outer planetary system and on its early evolution. We outline a scenario of primordial sculpting – issued from a combination of mechanisms proposed by various authors – that seems to explain most of the observed properties of the Kuiper belt. Several aspects are not yet totally clear. But, for the first time, we have a view – if not of the detailed sculpture – at least of its rough cast.

1. Introduction

When Edgeworth and Kuiper conjectured the existence of a belt of small bodies beyond Neptune – the presently called Kuiper belt – they certainly were imagining a disk of planetesimals preserving the pristine conditions of the proto-planetary disk. But, since the first discoveries of trans-Neptunian objects, astronomers have realized that this picture is not correct: the disk has been affected by a number of processes which have altered its original structure. The Kuiper belt may thus provide us with a large number of clues to understand what happened in the outer solar system during the primordial ages. Potentially, the Kuiper belt might teach us more about the formation of the giant planets than the planets themselves. And, as in a domino game, a better knowledge of giant planets formation would inevitably boost our understanding of the subsequent formation of the Solar System as a whole. Consequently, Kuiper belt research is now considered a top priority of modern planetary science.

Earth, Moon and Planets **92:** 1–27, 2003.

A decade after the discovery of 1992 QB_1 (Jewitt and Luu, 1993), we now know 770 trans-Neptunian objects (semi-major axis $a > 30$ AU)*. Of these, 362 have been observed during at least 2 oppositions, and 239 during at least three oppositions. Observations at 2 and 3 oppositions are necessary for the Minor Planet Center to compute the objects' orbital elements with, respectively, moderate and good accuracy. Therefore, the trans-Neptunian population is gradually taking shape, and we can start to seriously examine the Kuiper belt structure and learn what it has to teach us. We should not forget, however, that our view of the trans-Neptunian population is still partial, and strongly biased by a number of factors, some of which cannot be easily modeled.

A primary goal of this chapter is to present the orbital structure of the Kuiper belt as it stands from the current observations. We start in Section 2 by presenting the various sub-classes that constitute the trans-Neptunian population. Then in Section 3 we describe some striking properties of the population, such as its mass deficit, inclination excitation, radial extent and a puzzling correlation between orbital elements and physical properties. In Section 4 we combine some of the models that have been proposed so far on the primordial sculpting of the Kuiper belt, in order to outline a coherent scenario that might explain most of the observed properties of the Kuiper belt. The conclusions are in Section 5.

2. The Trans-Neptunian Populations

The trans-Neptunian population is "traditionally" subdivided in two sub-populations: the *scattered disk* and the *Kuiper belt*. The definition of these sub-populations is not unique, the Minor Planet Center and various authors often using slightly different criteria. Here we propose and discuss a partition based on the dynamics of the objects and their relevance for the reconstruction of the primordial evolution of the outer Solar System.

We call *scattered disk* the region of the orbital space that can be visited by bodies that have encountered Neptune within a Hill's radius at least once during the age of the Solar System, assuming no substantial modification of the planetary orbits. We then call *Kuiper belt* the complement of the scattered disk in the $a > 30$ AU region.

The bodies that belong to the scattered disk in this classification do not provide us any relevant clue to uncover the primordial architecture of the Solar System. In fact their current orbits might have been achieved starting from quasi-circular ones in Neptune's zone by pure dynamical evolution, in the framework of the current architecture of the solar system. The opposite is true for the orbits of the Kuiper belt objects. All bodies in the solar system must have been formed on orbits typical of an accretion disk (e.g. with very small eccentricities and inclinations). Therefore, the fact that most Kuiper belt objects have non-negligible eccentricity and/or

* All numbers are updated as of March 3, 2003.

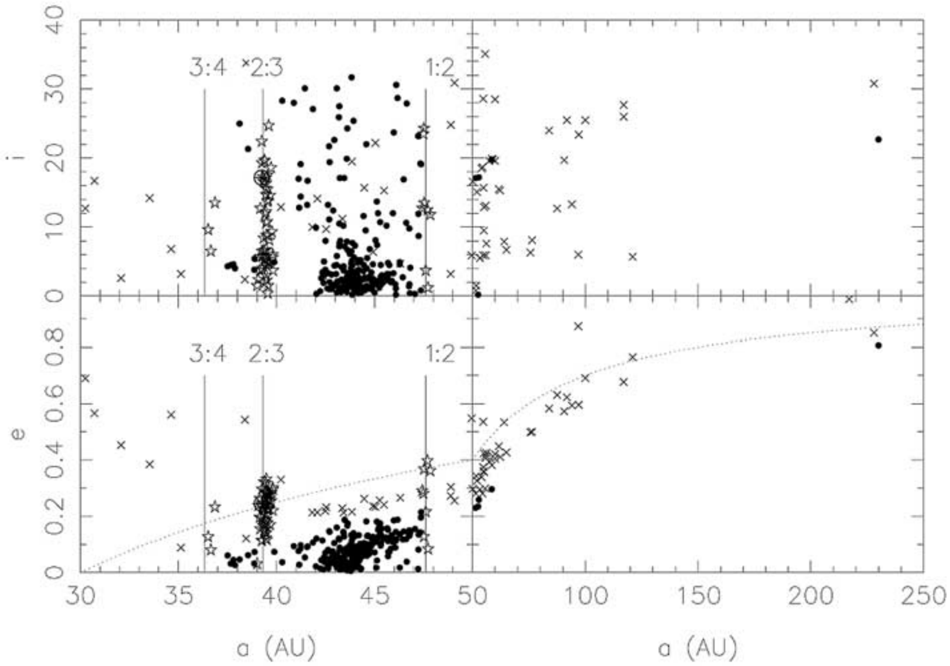

Figure 1. The orbital distribution of multi-opposition trans-Neptunian bodies, as of March 3, 2003. Scattered disk bodies are represented as a cross, classical Kuiper belt bodies as dots and resonant bodies as stars. We qualify that, in absence of long term numerical integrations of the evolution of all the objects and because of the uncertainties in the orbital elements, some bodies could have been miss-classified. Thus, the figure should be considered as an indicative representation of the various subgroups that compose the trans-Neptunian population. The dotted curve denotes $q = 30$ AU. The vertical solid lines mark the locations of the 3:4, 2:3 and 1:2 mean motion resonances with Neptune. The orbit of Pluto is represented by a crossed circle.

inclination reveals that some excitation mechanism, which is no longer at work, occurred in the past (see Section 4).

To categorize the observed trans-Neptunian bodies into scattered disk and Kuiper belt, we refer to previous works on the dynamics of trans-Neptunian bodies in the framework of the current architecture of the planetary system. For the $a < 50$ AU region, we use the results by Duncan et al. (1995) and Kuchner et al. (2002), who numerically mapped the regions of the (a, e, i) space with $32 < a < 50$ AU that can lead to a Neptune encountering orbit within 4 Gy. Because dynamics are reversible, these are also the regions that can be visited by a body after having encountered the planet. Therefore, according to our definition, they constitute the scattered disk. For the $a > 50$ AU region, we use the results by Levison and Duncan (1997) and Duncan and Levison (1997), who followed for another 4 Gy time-span the evolution of the particles that encountered Neptune in Duncan et al. (1995). Despite the fact that the initial conditions did not cover all possible configurations, we can reasonably assume that these integrations cumulatively show the regions of the orbital space that can be possibly visited by bodies transported to $a > 50$ AU by Neptune encounters. Again, according to our definition, these regions constitute the scattered disk.

In Figure 1 we show the (a, e, i) distribution of the trans-Neptunian bodies which have been observed during at least two oppositions. The bodies that belong to the scattered disk according to our criterion are represented as crosses. The Kuiper belt population is in turn subdivided in two sub-populations: the *resonant population* (star symbols in Figure 1) and the *classical belt* (dots). The former is made of the objects located in some major mean motion resonance with Neptune (essentially the 3:4, 2:3 and 1:2 resonances, but also the 2:5 – see Chiang et al., 2003), while the classical belt objects are not in any noticeable resonant configuration. It is well known that mean motion resonances offer a protection mechanism against close encounters with the resonant planet (Cohen and Hubbard, 1965). For this reason, the resonant population can have perihelion distances much smaller than the classical belt objects, and even Neptune-crossing orbits ($q < 30$ AU) as in the case of Pluto. The bodies in the 2:3 resonance are often called *Plutinos*, for the analogy of their orbit with that of Pluto.

Notice in Figure 1 also the existence of Kuiper belt bodies with $a > 50$ AU, on highly eccentric orbits: 5 objects currently known, including 2000CR$_{105}$ ($a =$ 230 AU, perihelion distance $q = 44.17$ AU and inclination $i = 22.7°$), but our classification is uncertain for the reasons explained in the figure caption). We call these objects *extended scattered disk* objects for three reasons: *(i)* they do not belong to the scattered disk according to our definition but are very close to its boundary; *(ii)* a body of $\sim$ 300 km like 2000CR$_{105}$ presumably formed much closer to the Sun, where the accretion timescale was sufficiently short (Stern, 1996), implying that it has been subsequently transported in semi-major axis until its current location was reached; *(iii)* the lack of objects with $q > 41$ AU and $50 < a < 200$ AU should not be due to observational biases, given that many classical belt objects have been discovered up to distances of 45–50 AU (see Figure 5), suggesting that the extended scattered disk objects are *not* the highest eccentricity members of an excited belt beyond 50 AU. These considerations indicate that in the past the true scattered disk extended well beyond its present boundary in perihelion distance. Why this was so, is particularly puzzling. Given that the observational biases become more severe with increasing perihelion distance and semi-major axis, the currently known extended scattered disk objects may be like the tip of an iceberg, e.g. the emerging representatives of a conspicuous population, possibly outnumbering the scattered disk population (Gladman et al., 2002).

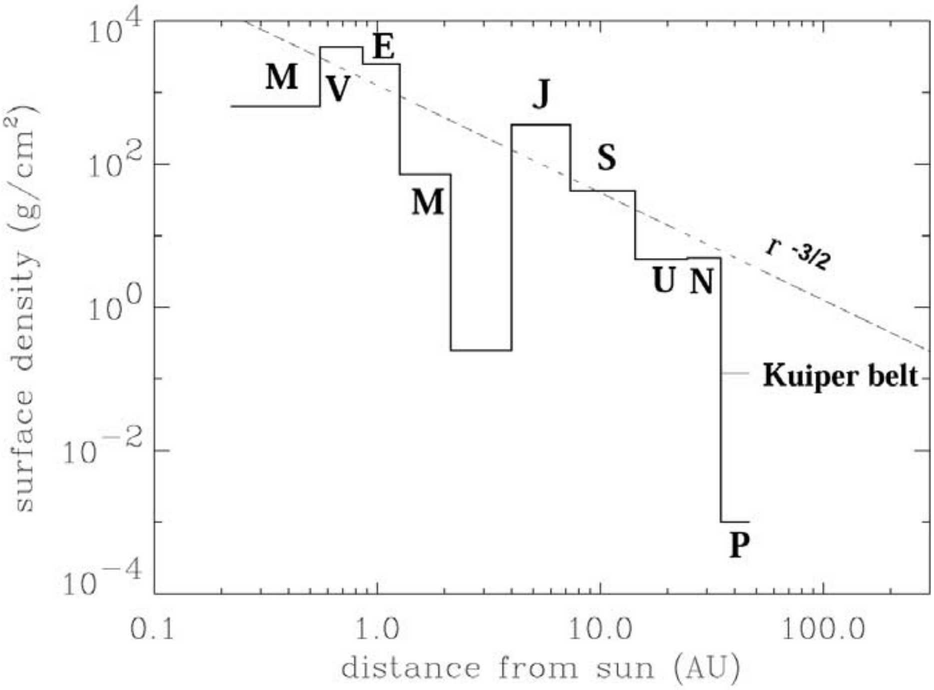

Figure 2. The mass distribution of the solar nebula inferred from the masses of the planets augmented by the mass needed to bring the observed material to solar composition (data from Lewis 1995). The surface density in the Kuiper belt has been computed assuming a current mass of $\sim 0.1\ M_{\oplus}$ (Jewitt et al., 1996; Chiang and Brown, 1999; Trujillo et al., 2001; Gladman et al., 2001) in the 42–48 AU annulus, and scaling the result by a factor 70 in order to account for the inferred primordial local ratio between volatiles and solids. The estimate of the total mass in the Kuiper belt overwhelms that of Pluto, but still does not bring the mass to the extrapolation of the $\sim r^{-3/2}$ line.

3. The Structure of the Kuiper Belt

3.1. The Missing Mass of the Kuiper Belt

The original argument followed by Kuiper (1951) to conjecture the existence of a band of small planetesimals beyond Neptune was related to the mass distribution in the outer solar system. The minimum mass solar nebula inferred from the total planetary mass (plus lost volatiles) smoothly declines from the orbit of Jupiter until the orbit of Neptune (see Figure 2); why should it abruptly drop beyond the last planet? However, while Kuiper's conjecture on the existence of a trans-Neptunian belt is correct, the total mass in the 30–50 AU range inferred from observations is two orders of magnitude smaller than the one he expected.

Kuiper's argument is not the only indication that the mass of the primordial Kuiper belt had to be significantly larger. Further evidence for a massive primordial Kuiper belt was uncovered by Stern (1995) who found that the objects currently in the Kuiper belt were incapable of having formed in the present environment: collisions are sufficiently infrequent that 100 km objects cannot be built by pairwise accretion of the current population over the age of the solar system. Moreover, owing to the large eccentricities and inclinations of Kuiper belt objects – and consequently to their high encounter velocities – collisions that do occur tend to be erosive rather than accretional, making bodies smaller rather than larger. Stern suggested that the resolution of this dilemma is that the primordial Kuiper belt was both more massive and dynamically colder, so that more collisions occurred, and they were gentler and therefore generally accretional.

Following this idea, detailed modeling of accretion in a massive primordial Kuiper belt was performed by Stern (1996), Stern & Colwell (1997a,b) and Kenyon and Luu (1998, 1999a, 1999b). While each model includes different aspects of the relevant physics of accretion, fragmentation, and velocity evolution, the basic results are in approximate agreement. First, with $\sim$10 $M_\oplus$ (Earth masses) or more of solid material in an annulus from about 35 to 50 AU on very low eccentricity orbits ($e \leq 0.001$), all models naturally produce of order a few objects the size of Pluto and approximately the right number of $\sim$ 100km objects, on a timescale ranging from several 10^7 to several 10^8 y. The models suggest that the majority of mass in the disk was in bodies approximately 10km and smaller. The accretion stopped when the formation of Neptune or other dynamical phenomena (see section 4) began to induce eccentricities and inclinations in the population high enough to move the collisional evolution from the accretional to the erosive regime (Stern 1996).

A massive and dynamically cold primordial Kuiper belt is also required by the models that attempt to explain the formation of the observed numerous binary Kuiper belt objects (Goldreich et al., 2002; Weidenshilling, 2002).

Therefore, the general formation picture of an initial massive Kuiper belt appears secure, and understanding the ultimate fate of the 99% of the initial Kuiper belt mass that appears to be no longer in the Kuiper belt is a crucial step in reconstructing the history of the outer solar system.

3.2. THE EXCITATION OF THE KUIPER BELT

An important clue to the history of the early outer solar system is the dynamical excitation of the Kuiper belt. While eccentricities and inclinations of resonant and scattered objects are expected to have been affected by interactions with Neptune, those of the classical objects should have suffered no such excitation. Nonetheless, the confirmed classical belt objects have an inclination range up to at least 32 degrees and an eccentricity range up to 0.2, significantly higher than expected from a primordial disk, even accounting for mutual gravitational stirring.

The observed distributions of eccentricities and inclinations in the Kuiper belt are highly biased. High eccentricity objects have closer approaches to the Sun and thus become brighter and more easily detected. High inclination objects spend little time at low latitudes* at which most surveys take place, while low inclination objects spend zero time at the high latitudes where some searches have occurred.

Determination of the eccentricity distribution of the Kuiper belt requires disentanglement of eccentricity and semi-major axis, which is only possible for objects with well determined orbits, for which a large enough well-characterized sample is not yet available. Determination of the inclination distribution, however, is much simpler because the inclination of an object is well determined even after a small number of observations, and the latitude of discovery of each object is a known quantity. Using these facts, Brown (2001) developed general methods for debiasing object discoveries to discern the underlying inclination distribution. The simplest method removes the latitude-of-discovery biases by considering only objects discovered within one degree of the invariable plane equator and weights each object by $\sin(i)$, where i is the inclination of each object, to account for the proportional fraction of time that objects of different inclination spend at the equator (strictly, one should use only objects found precisely at the equator; expanding to one degree around the equator greatly increases the sample size while biasing the sample slightly against objects with inclinations between 0 and 1 degree). An important decision to be made in constructing this inclination distribution is the choice of which objects to include in the sample. One option is to use only confirmed classical objects, by which we mean those that have been observed at least 2 oppositions and for which the orbit is reasonably assured of fitting the definition of the classical Kuiper belt, as defined above. The possibility exists that these objects are biased in some way against unusual objects which escape recovery at a second opposition because of unexpected orbits, but we expect that this bias is likely to be in the direction of under-reporting high inclination objects. On the other hand, past experience has shown that if we use all confirmed and unconfirmed classical bodies, we pollute the sample with misclassified resonant and scattered objects, which generally have higher inclinations and therefore artificially inflate the inclination distribution of the classical belt. We therefore chose to use only confirmed classical belt bodies with the caveat that some high inclination objects might be missing. Figure 3 shows the inclination distribution of the classical Kuiper belt derived from this method. This method has the advantage that it is simple and model independent, but the disadvantage that it makes no use of the information contained in high latitude surveys where most of the high inclination objects are discovered. For example, the highest inclination classical belt body found within 1 degree of the equator has an inclination of 10.1 degrees, while an object with an inclination of 31.9 degrees has been found at a latitude of 11.2 degrees. The two high inclination points in Figure 3 attempt to partially correct this deficiency by using discoveries of objects between 3 and 6 degrees latitude to define the high inclination end of the inclination distribution, using Equation (3) of Brown (2001).

* Latitude and inclination are defined with respect to the invariable plane, which is a better representation for the plane of the Kuiper belt than is the ecliptic (Brown and Trujillo, 2003).

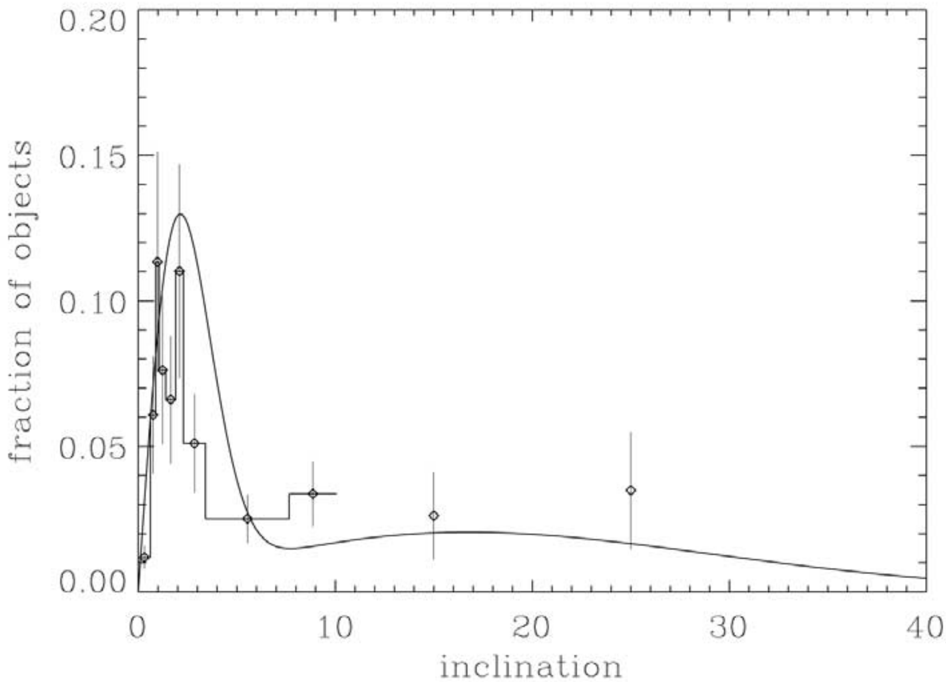

Figure 3. The inclination distribution (in deg.) of the classical Kuiper belt. The points with error bars show the model-independent estimate constructed from a limited subset of confirmed classical belt bodies, while the smooth line shows the best fit two population model $f(i)di = \sin(i)[96.4 \exp(-i^2/6.48) + 3.6 \exp(-i^2/288)]di$ (Brown, 2001). In this model ~60% of the objects have $i > 4°$.

Observations at these latitudes miss all objects with lower inclinations, but we can linearly scale the high latitude distribution to match the low latitude distribution in the region where they are both valid from 6 to 10 degrees and retrive a correctly relatively calibrated high inclination distribution.

A clear feature of this modeled distribution is the presence of distinct high and low inclination populations. While Brown (2001) concluded that not enough data existed at the time to determine if the two populations were truly distinct or if the model fit forced an artificial appearance of two populations, the larger amount of data now available, and shown in the model-independent analysis of Figure 3, confirms that the distinction between the populations is real. The sharp drop around 4 degrees is independent of any model, while the extended distribution to 30 degrees is demanded by the presence of objects with these inclinations.

3.3. Physical evidence for two populations in the classical belt

The existence of two distinct classical Kuiper belt populations, which we will call the hot ($i > 4$) and cold ($i < 4$) classical populations, could be caused in one of two general manners. Either a subset of an initially dynamically cold population was excited, leading to the creation of the hot classical population, or the populations are truly distinct and formed separately. One manner in which we can attempt to determine which of these scenarios is more likely is to examine the physical properties of the two classical populations. If the objects in the hot and cold populations are physically different it is less likely that they were initially part of the same population.

The first suggestion of a physical difference between the hot and the cold classical objects came from Levison and Stern (2001) who noted that the intrinsically brightest classical belt objects (those with lowest absolute magnitudes) are preferentially found with high inclination. Trujillo and Brown (2003) have recently verified this conclusion in a bias-independent manner from a survey for bright objects which covered $\sim$70% of the ecliptic and found many hot classical objects but few cold classical objects.

The second possible physical difference between hot and cold classical Kuiper belt objects is their colours, which relates in an unknown manner to surface composition. Several possible correlations between orbital parameters and colour were suggested by Tegler and Romanishin (2000) and further investigated by Doressoundiram et al. (2001). The issue was clarified by Trujillo and Brown (2002) who quantitatively showed that for the classical belt, inclination, and no other independent orbital parameter, is correlated with colour. In essence, the low inclination classical objects tend to be redder than higher inclination objects. Hainaut (2002) has compiled a list of all published Kuiper belt colours which more than doubles the sample of Trujillo and Brown.

More interestingly, we see that the colours naturally divide into distinct low inclination and high inclination populations at precisely the location of the divide between the hot and cold classical objects. These populations differ at a 99.9% confidence level. Interestingly, the cold classical population also differs in colour from the Plutinos and the scattered objects at the 99.8% and 99.9% confidence level, respectively, while the hot classical population appears identical in colour to these other populations. The possibility remains, however, that the colours of the objects, rather than being markers of different populations, are actually *caused* by the different inclinations. Stern (2002), for example, has suggested that the higher average impact velocities of the high inclination objects will cause large scale resurfacing by fresh water ice which could be blue to neutral in colour. However, a careful analysis shows that there is clearly no correlation between average impact velocity and colour (Thebault and Doressoundiram, 2003).

In summary, the significant colour and size differences between the hot and cold classical objects imply that these two populations are physically different in addition to being dynamically distinct.

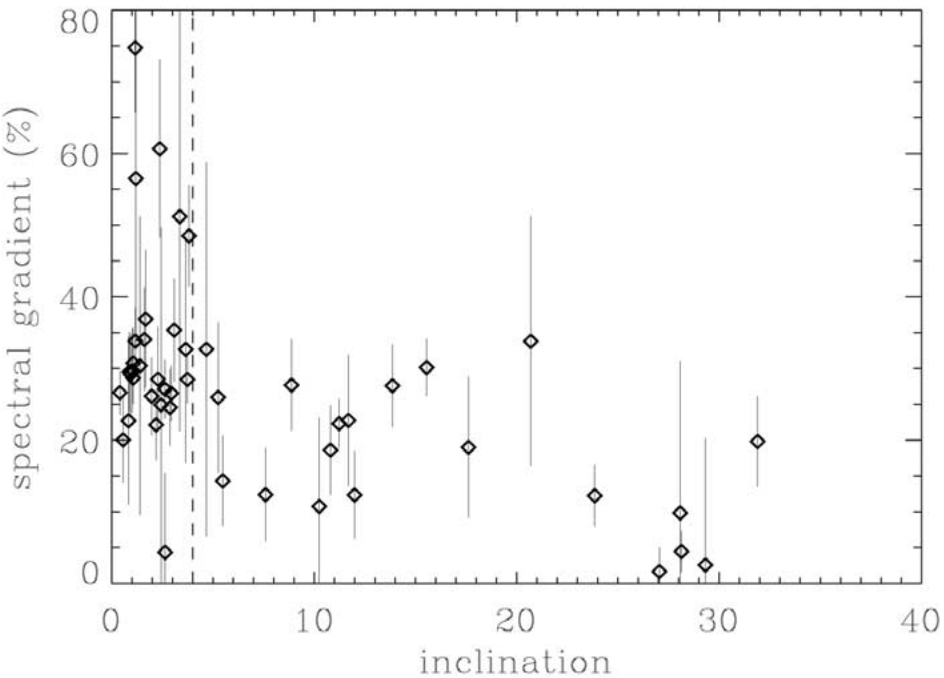

Figure 4. Colour gradient versus inclination in the classical Kuiper belt. Colour gradient is the slope of the spectrum, in % per 100 nm, with 0% being neutral and large numbers being red. The hot and cold classical objects have significantly different distributions of colour.

3.4. THE RADIAL EXTENT OF THE KUIPER BELT

Another important property of interest for understanding the primordial evolution of the Kuiper belt is its radial extent. While initial expectations were that the mass of the Kuiper belt should smoothly decrease with heliocentric distance – or perhaps even increase in number density by a factor of $\sim$100 back to the level of the extrapolation of the minimum mass solar nebula beyond the region of Neptune's influence (Stern, 1996) – the lack of detection of objects beyond about 50 AU soon began to suggest a drop off in number density (Dones, 1997; Jewitt et al., 1998; Chiang and Brown, 1999; Trujillo et al., 2001; Allen et al., 2001). It was often argued that this lack of detections was the consequence of a simple observational bias caused by the extreme faintness of objects at greater distances from the sun (Gladman et al., 1998), but Allen et al. (2001, 2002) showed convincingly that for a fixed absolute magnitude distribution, the number of objects with semimajor axis less than 50 AU was larger than the number greater than 50 AU and thus some density decrease was present.

Determination of the magnitude of the density drop beyond 50 AU was hampered by the small numbers of objects and thus weak statistics in individual surveys. Trujillo and Brown (2001) developed a method to use all detected objects to estimate a radial distribution of the Kuiper belt. The method relies on the fact that the heliocentric distance (*not* semi-major axis) of objects, like the inclination, is well determined in a small number of observations and that within ∼100 AU surveys have no biases against discovering distant objects other than the intrinsic radial distribution and the easily quantifiable brightness decrease with distance. Thus, at a particular distance, a magnitude m_0 will correspond to a particular object diameter s, but, assuming a power-law differential size distribution, each detection of an object of diameter s can be converted to an equivalent number n of objects of diameter s_0 by $n = (s/s_0)^{q-1}$ where q is the differential power-law size index. Thus the observed radial distribution of objects with magnitude m_0, $O(r, m_0)dr$ can be converted to the true radial distribution of objects of diameter s_0 by

$$R(r, s_0)dr = O(r, m_0)dr \left[\frac{r(r-1)10^{(m_0-24.55)/5}}{15.60 s_0} \right]^{q-1},$$

where albedos of 4% are assumed, but only enter as a scaling factor. Measured values of q for the Kuiper belt have ranged from 3.5 to 4.8 (see Trujillo and Brown (2001) for a review). We will assume the steepest currently proposed value of $q = 4.45$ (Gladman et al., 2001), which puts the strongest constraints on the existence of distant objects.

Figure 5 shows the total equivalent number of 100 km diameter objects as a function of distance implied by the detection of the known trans-Neptunian objects. Note that no error bars appear here because the only statistically meaningful method to determine errors is to compare the observed radial distribution to the distribution that would be expected to be observed with hypothetical distributions. That analysis is carried out below. One small improvement has been made to the Trujillo and Brown (2001) method. The power law size distribution is only assumed to be valid from 50 to 1000 km in diameter, corresponding to an expected break in the power law at some small diameter (Kenyon and Luu, 1999a) and a maximum object's size. The effect of this change is to only use objects between magnitudes 22.7 and 24.8, which makes the analysis only valid from 30 AU (where a 50 km object would be magnitude 24.8) to 80 AU (where a 1000 km object would be magnitude 22.7). Changes in the maximum object size assumed, $s_{\max}$ are equivalent to changing the outer limit of the validity of the analysis by $80\text{AU}(s_{\max}/1000\text{km})^{1/2}$. Alternatively, one could further restrict the magnitude limits considered to limit the maximum size while maintaining validity to a particular distance. Different choices of minimum and maximum diameters have little effect on the final result unless extreme values for the maximum are chosen.

The analysis clearly shows that the known Kuiper belt is a localized increase in number density. Several implicit assumptions go into the above method, but only extreme changes in these assumptions substantially change the results. For example, a change in the object size distribution beyond 43 AU could mimic a drop in object number density, but only if, by 50 AU, the distribution is so extreme

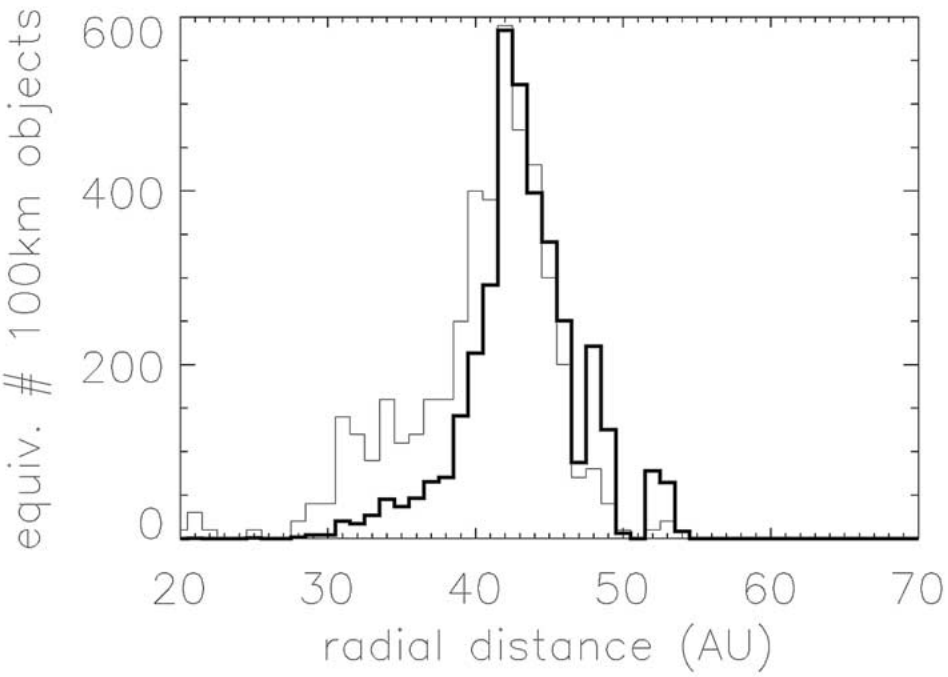

Figure 5. The radial distribution of the Kuiper belt. The light line shows the observed number of trans-Neptunian objects per AU interval (times ten), while the thick bold line shows the true radial distribution (of 100 km diameter objects) inferred from this observed distribution taking into account biases due to brightness, distance, and diameter of the object. All discovered trans-Neptunian objects are considered in this analysis, regardless of their dynamical class.

that most of the mass is either in a few (undiscovered) large objects or a large number of (too faint) small objects. A physical reason for such a change is not apparent. Likewise, a lowering of albedo beyond 50 AU could make the appearance of a drop in number density, but, again, such a lowering is not physically motivated. A change in the inclination distribution beyond 50 AU could have the effect of hiding objects if they are concentrated in low inclination orbits close to the invariable plane, but repeating the analysis considering only objects found within 1 degree of the invariable plane still shows the sharp drop. While changing of these assumptions could indeed invalidate the analysis method above, the much simpler conclusion is that the number density of the Kuiper belt peaks strongly at 42 AU and quickly drops off beyond.

While the Trujillo and Brown (2001) method is good at giving an indication of the radial structure of the Kuiper belt where objects have been found, it is less good at determining upper limits to the detection of objects where none have been found. A simple extension, however, allows us to easily test hypothetical radial distributions against the known observations by looking at observed radial distributions of all objects found at a particular magnitude m_0 independent of any knowledge of how these objects were found. Assume a true radial distribution of objects $R(r)dr$ and again assume the above power law differential size distribution and maximum size. For magnitudes between m and $m + dm$, we can construct the expected observed radial distribution of all objects found at that magnitude, $o(r, m)drdm$ by

$$o(r, m)drdm = R(r)dr\left[\frac{r(r-1)10^{(m-24.55)/5}}{15.6s_0}\right]^{-q+1} dm,$$

where r ranges from that where the object of brightness m has a diameter of 50 km (corresponding to the hypothesized break in the power-law size distribution) to that where the object of brightness m has a diameter of $s_{\max}$. We assume a diameter of $s_{\max} = 1000$ km in the analysis below. The overall expected observed radial distribution is then simply the sum of $o(r, m)$ over the values of m corresponding to all detected objects. We can then apply a K-S test to determine the probability that the observed radial distribution could have come from the modeled radial distribution. We first apply this test to determine the magnitude of the drop off beyond 42 AU. Standard assumptions about the initial solar nebula suggest a surface density drop off of $r^{-3/2}$. Figure 6 shows the observed radial distribution of objects compared to that expected if the surface density of objects dropped off as $r^{-3/2}$ beyond 42 AU. This distribution can be ruled out at the many sigma level. Assuming that the surface density drops as some power law, we model a range of different distribution $r^{-\alpha}$ and find a best fit of $\alpha = -11 \pm 4$ where the error bars are 3σ. This radial decay function should presumably hold up to ~ 60 AU, beyond which we expect to encounter a much flatter distribution due to the scattered disk objects.

It has been conjectured that beyond some range of Neptune's influence the number density of Kuiper belt objects could increase back up to the level expected for the minimum mass solar nebula (Stern, 1996; see Section 3.1). We therefore model a case where the Kuiper belt from 42 to 60 AU falls off as r^{-11} but beyond that the belt reappears at a certain distance δ with a number density found by extrapolating the $r^{-3/2}$ power law from the peak density at 42 AU and multiplying by 100 to compensate for the mass depletion of the classical belt (Figure 6). Such a model of the radial distribution of the Kuiper belt can be ruled out at the 3σ level for all δ less than 115 AU (around this distance biases due to the slow motions of these objects also become important, so few conclusion can be drawn from the current data about objects beyond this distance). If the model is slightly modified to make the maximum object mass proportional to the surface density at a particular radius, a 100 times resumption of the Kuiper belt can be ruled out inside 94 AU. Similar models can be made where a gap in the Kuiper belt exists at the presently observed location but the belt resumes at some distance with no extra enhancement in number density. These models can be ruled out inside 60 AU at a 99% confidence level.

While all of these results are necessarily assumption dependent, several straightforward interpretations are apparent. First, the number density of Kuiper belt

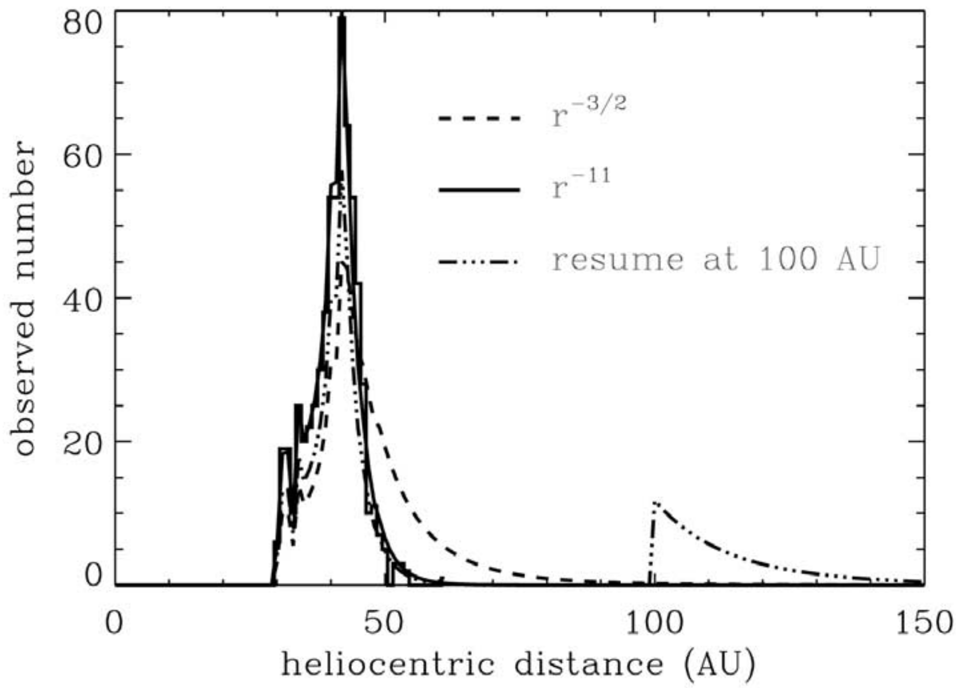

Figure 6. The observed radial distribution of Kuiper belt objects (solid histogram) compared to observed radial distributions expected for models where the surface density of Kuiper belt objects decreases by $r^{-3/2}$ beyond 42 AU (dashed curve), where the surface density decreases by r^{-11} beyond 42 AU (solid curve), and where the surface density at 100 AU increases by a factor of 100 to the value expected from an extrapolation of the minimum mass solar nebula (dashed-dotted curve).

objects drops sharply from its peak at around 42 AU. Second, a distant Kuiper belt with a mass approaching that of the minimum mass solar nebula is ruled out inside at least ∼100 AU. And finally, a resumption of the Kuiper belt at a density of about 1% expected from a minimum mass solar nebula is ruled out inside ∼ 60 AU.

4. The Primordial Sculpting of the Kuiper Belt

The previous section makes clear than the Kuiper belt has lost, sometime during the solar system history, the structure of an accretional disk (very small e and i) that presumably it had in the past.

A large number of mechanisms have been proposed so far to explain some of the observational properties of the Kuiper belt. For space limitation we debate here only those which in our opinion – at the light of our current observational knowledge of the Kuiper belt – played a role in in the primordial sculpting of the

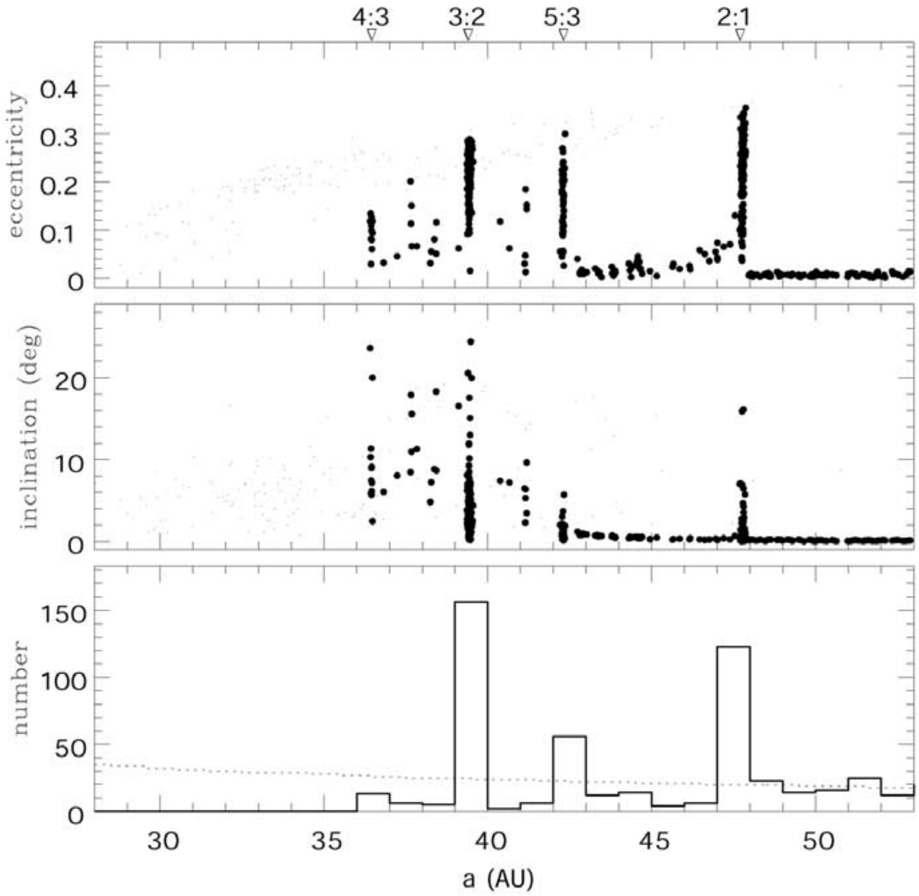

Figure 7. Final distribution of the Kuiper belt bodies according to the sweeping resonances scenario (courtesy of R. Malhotra). The simulation is done by numerical integrating, over a 200 Myr timespan, the evolution of 800 test particles on initial quasi–circular and coplanar orbits. The planets are forced to migrate (Jupiter: -0.2 AU;, Saturn: 0.8 AU; Uranus: 3 AU; Neptune: 7 AU) and reach their current orbits on an exponential timescale of 4 Myr. Large solid dots represent 'surviving' particles (i.e., those that have not suffered any planetary close encounters during the integration time); small dots represent the 'removed' particles at the time of their close encounter with a planet. In the lowest panel, the solid line is the histogram of semi-major axis of the 'surviving' particles; the dotted line is the initial distribution

trans-Neptunian population. A more exhaustive review can be found in Morbidelli and Brown (2003).

4.1. Origin of the resonant populations

Fernández and Ip (1984) showed that, while scattering primordial planetesimals, Neptune should have migrated outwards. Malhotra (1993, 1995) realized that, following Neptune's migration, the mean motion resonances with Neptune also migrated outwards, sweeping the primordial Kuiper belt until they reached their present position. From adiabatic theory (Henrard, 1982), some of the Kuiper belt objects swept by a mean motion resonance would have been captured into resonance; they would have subsequently followed the resonance in its migration, while increasing their eccentricity. This model accounts for the existence of the large number of Kuiper belt objects in the 2:3 mean motion resonance with Neptune (and also in other resonances) and explains their large eccentricities (see Figure 7). Reproducing the observed range of eccentricities of the resonant bodies requires that Neptune migrated by 7 AU. Malhotra's simulations also showed that the bodies captured in the 2:3 resonance can acquire large inclinations, comparable to that of Pluto and other objects. The mechanisms that excite the inclination during the capture process have been investigated in detail by Gomes (2000), who concluded that, although large inclinations can be achieved, the resulting proportion between the number of high inclination vs. low inclination bodies and their distribution in the eccentricity vs. inclination plane do not reproduce well the observations. According to Gomes (2003) most high inclination Plutinos were captured during Neptune's migration from the scattered disk population, rather than from an originally cold Kuiper belt as in Malhotra scenario.

The mechanism of adiabatic capture into resonance requires that Neptune's migration happened very smoothly. If Neptune had encountered a significant number of large bodies (Lunar mass or more), its jerky migration would have jeopardized capture into resonances. Hahn and Malhotra (1999), who simulated Neptune's migration using a disk of Lunar to Martian-mass planetesimals, did not obtain any permanent capture. The precise constraints set by the capture process on the size distribution of the largest disk's planetesimals have never been quantitatively computed, but they are likely to be severe.

4.2. Origin of the Hot Population

An appealing mechanism for the origin of the hot population has been proposed by Gomes (2003), also in the framework of the planetary migration scenario. Like Hahn and Malhotra (1999) Gomes simulated Neptune's migration, starting from about 15 AU, by the interaction with a massive planetesimal disk extending from beyond Neptune's initial position. But, taking advantage of the improved computer technology, he used 10,000 particles to simulate the disk population, with individual masses roughly equal to twice the Pluto's mass, while Hahn and Malhotra used only 1,000 particles, with Lunar to Martian masses. In his simulations, during its migration Neptune scattered the planetesimals and formed a massive scattered disk. Some of the scattered bodies decoupled from the planet, by decreasing their eccentricity through the interaction with some secular or mean-motion resonance. If Neptune had not been migrating, as in Duncan and Levison (1997) integrations, the decoupled phases would have been transient, because the eccentricity would have eventually increased back to Neptune-crossing values, the dynamics being

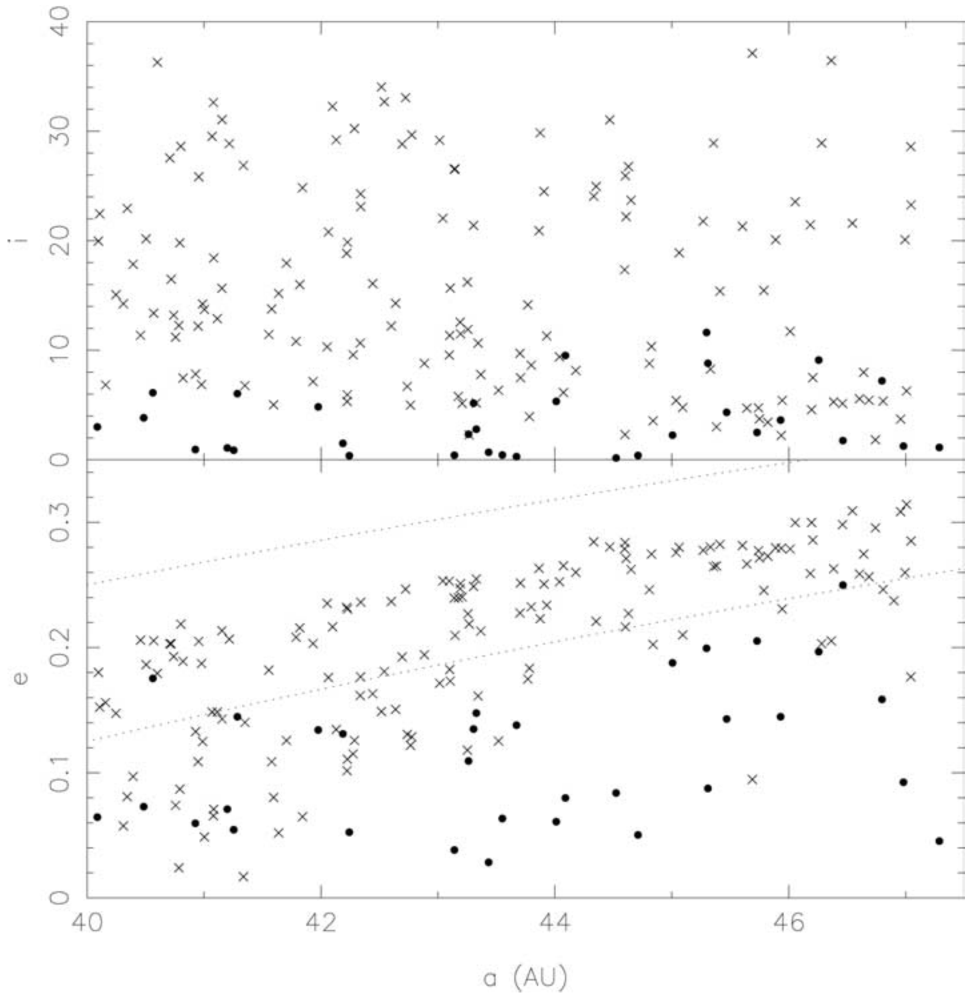

Figure 8. The orbital distribution in the classical belt according to Gomes' simulations. The dots denote the local population, which is only moderately dynamically excited. The crosses denote the bodies that were originally inside 30 AU. Therefore, the resulting Kuiper belt population is the superposition of a dynamically cold population and of a dynamically hot population, which gives a bi-modal inclination distribution comparable to that observed. The dotted curves in the eccentricity vs. semi-major axis plot correspond to $q = 30$ AU and $q = 35$ AU. Courtesy of R. Gomes.

reversible. But Neptune's migration broke the reversibility, and some of the decoupled bodies managed to escape from the resonances, and remained permanently trapped in the Kuiper belt. As shown in Figure 8, the current Kuiper belt would therefore be the result of the superposition of these bodies with the local population, originally formed beyond 30 AU, which stays dynamically cold because only moderately excited (by the resonance sweeping mechanism, as in Figure 7).

The migration mechanism is sufficiently slow (several 10^7 y) that the scattered particles have the time to acquire very large inclinations, consistent with the observed hot population. The resulting inclination distribution of the bodies in the classical belt is bimodal, and quantitatively reproduces the de-biased inclination distribution computed by Brown (2001) from the observations.

In Gomes (2003) simulations an extended scattered disk is also formed beyond 50 AU. Although bodies on orbits similar to that of 2000 CR_{105} are not obtained in the nominal simulations, other tests done in Gomes (2003) and the new simulations presented by Gomes in this book are suggestive that such orbits could be achieved in the framework of the same scenario.

Assuming that the bodies' colour varied in the primordial disk with heliocentric distance, Gomes scenario also explains why the scattered objects, and hot classical belt objects, which mostly come from regions inside ∼30 AU, appear to have similar colour distributions, while the cold classical objects – the only ones that actually formed in the trans-Neptunian region – have a different distribution. The Plutinos would be a mixture of the two populations. Similarly, assuming that the maximal size of the objects was a decreasing function of the heliocentric distance at which they formed, Gomes scenario also explains why the biggest Kuiper belt objects are all at large inclination.

4.3. Origin of the outer edge of the Kuiper belt

The existence of an outer edge of the Kuiper belt is a very intriguing property. At least three mechanisms for its origin have been proposed, none of which has raised the general consensus of the community of the experts.

Brunini and Melita (2002) showed with numerical simulations that a Martian mass body residing for 1 Gy on an orbit with $a \sim 60$ AU and $e \sim 0.15$–0.2 could have scattered into Neptune-crossing orbits most of the Kuiper belt bodies originally in the 50–70 AU range, leaving this region strongly depleted and dynamically excited. As shown in Figure 6 the apparent edge at 50 AU might be simply the inner edge of a similar gap in the distribution of Kuiper belt bodies. A problem of the Brunini and Melita scenario is that there are no evident dynamical mechanisms that would ensure the later removal of the massive body from the system. In other words, the massive body should still be present, somewhere in the $\sim 50 - 70$ AU region. A Mars-size body with 4% albedo at 70 AU would have apparent magnitude brighter than 20, so that, if its inclination is small ($i < 10°$) it is unlikely that it escaped detection in the numerous wide field ecliptic surveys that have been performed up to now, and in particular in that led by Trujillo and Brown (2003). We remark that a small inclination should be expected if the putative Matian body was originally a scattered disk object whose eccentricity (and inclination) were damped by dynamical friction (as conjectured by Brunini and Melita) or if it reached its required heliocentric distance by migrating through the primordially massive Kuiper belt (the most likely evolution according to Gomes et al., 2003).

Weidenschilling (2003) suggested that the outer edge of the Kuiper belt be the result of the facts that accretion takes longer with increasing heliocentric distance and small planetesimals drift inwards due to gas drag. This leads to a steepening of the radial surface density gradient of solids. The edge effect is augmented because, at whatever distance large bodies can form, they capture the ∼m-sized bodies spiraling in from farther out. The net result of the process, as shown by Weidenschilling's numerical modeling, is production of an edge, where both the surface density of solid matter and the mean size of planetesimals decrease sharply with distance.

A third possibility is that the planetesimal disk was truncated by the passage of a star in the vicinity of the Sun. Ida et al. (2000) and Kobayashi and Ida (2001) showed that the resulting eccentricities and inclinations of the planetesimals would depend critically on a/D, where a is their semi-major axis and D is the heliocentric distance of the stellar encounter. A stellar encounter at $\sim$ 200 AU would make most of the bodies beyond 50 AU so eccentric to intersect the orbit of Neptune, which eventually would produce the observed edge (Melita et al., 2002). An interesting constraint on the time at which such an encounter occurred is set by the existence of the Oort cloud. Levison et al. (2003) showed that the encounter had to occur much earlier than $\sim$ 10 My after the formation of Uranus and Neptune, otherwise most of the existing Oort cloud would have been ejected to interstellar space and many of the planetesimals in the scattered disk would have had their perihelion distance lifted beyond Neptune, decoupling from the planet. As a consequence, the extended scattered disk population, with $a > 50$ AU and $40 < q < 50$ AU, would have had a mass comparable or larger than that of the resulting Oort cloud, hardly compatible with the few detections of extended scattered disk objects performed up to now. An encounter with a star during the first million year from planetary formation is a likely event if the Sun formed in a stellar cluster (Bate et al., 2003). At such an early time, presumably the Kuiper belt objects were not yet fully formed (Stern, 1996; Kenyon and Luu, 1998). In this case, the edge of the belt would be at a heliocentric distance corresponding to a post-encounter eccentricity excitation of $\sim$ 0.05, a threshold value below which collisional damping is efficient and accretion can recover, and beyond which the objects rapidly grind down to dust (Kenyon and Bromley, 2002).

The edge-forming stellar encounter could not be the responsible for the origin of the peculiar orbit of 2000 CR_{105}. In fact, such a close encounter would produce also a relative overabundance of bodies with perihelion distance similar to that of 2000 CR_{105} but with semi-major axis in the 50–200 AU range. These bodies have never been discovered despite of the more favorable observational biases. In order that only bodies with $a > 200$ AU have their perihelion distance lifted, a second stellar passage at about 800 AU is required (Morbidelli and Levison, 2003). Interestingly, from the analysis of the Hipparcos data, Garcia-Sanchez et al. (2001)

concluded that, with the current stellar environment, the closest encounter with a star during the age of the solar system would be at $\sim$ 900 AU.

4.4. THE MASS DEFICIT OF THE COLD POPULATION

The scenario proposed by Gomes (2003) reduces the problem of the mass depletion of the Kuiper belt to the sole cold population. In fact, in Gomes' simulations, only $\sim$0.2% of the bodies initially in the disk swept by Neptune remained in the Kuiper belt on stable high-i orbits at the end of Neptune's migration, which naturally explains the current low mass of the hot population. However, the population originally in the 40-50 AU range – which would constitute the cold population in Gomes scenario – should have been only moderately excited and not dynamically depleted, so that it should have preserved most of its primordial mass.

Two general mechanisms have been proposed for the mass depletion: the dynamical ejection of most of the bodies from the Kuiper belt to the Neptune-crossing region and the collisional comminution of most of the mass of the Kuiper belt into dust.

The dynamical depletion mechanism was proposed by Morbidelli and Valsecchi (1997) and Petit et al. (1999). In their scenario, planetary embryos, with mass comparable to that of Mars or of the Earth, was scattered by Neptune onto a high-eccentricity orbit that crossed the Kuiper belt for $\sim 10^8$ y. The repeated passage of the embryo through the Kuiper belt excited the eccentricities of the Kuiper belt bodies, the vast majority of which became Neptune crossers and were subsequently dynamically eliminated by the planets' scattering action. In the Petit et al. (1999) integrations that supported this scenario, however, the Kuiper belt bodies were treated as test particles, and therefore their ejection to Neptune-crossing orbit did not alter the position of Neptune. Gomes et al. (2003) have re-done a Petit et al.-like simulations in the framework of a more self-consistent model accounting for planetary migration. As expected, the dynamical depletion of the Kuiper belt largely enhances Neptune's migration. The reason for this is that, thanks to the dynamical excitation of the distant disk provided by the embryo, Neptune interacts not only with the portion of the disk in its local neighborhood, but with the entire mass of the disk at the same time. As shown in Figure 9 even a low mass disk of 30 $M_\oplus$ between 10 and 50 AU (7.5 $M_\oplus$ in the Kuiper belt) drives Neptune well beyond 30 AU. Halting Neptune's migration at $\sim$ 30 AU requires a disk mass of $\sim 15 M_\oplus$ or less (depending on the initial Neptune's location). Such a mass and density profile would imply only 3.75 $M_\oplus$ of material originally in the Kuiper belt between 40 and 50 AU, which is less than the mass required (10–30 $M_\oplus$) by the models of accretion of Kuiper belt bodies (Stern and Colwell, 1997; Kenyon and Luu, 1999).

A priori, for what concerns Neptune's migration, there is no evident difference between the case where the Kuiper belt is excited to Neptune-crossing orbit by a planetary embryo or by some other mechanism, such as the primordial secular

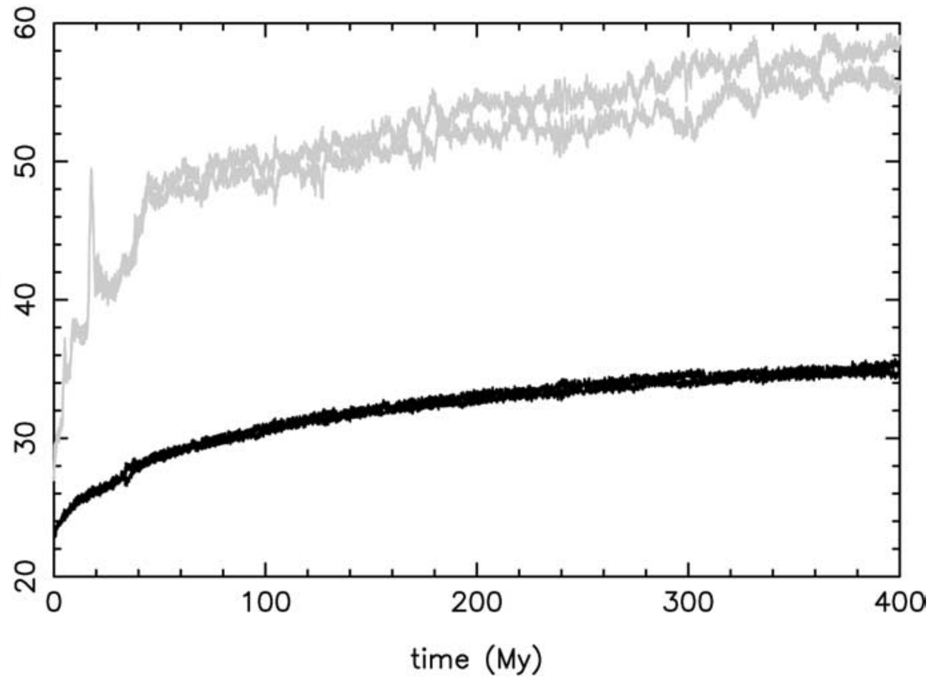

Figure 9. A self-consistent simulation of the Petit et al. (1999) scenario for the excitation and dynamical depletion of the Kuiper belt (from Gomes et al., 2003). Neptune is originally assumed at $\sim$ 23 AU and an Earth-mass embryo at $\sim$ 27 AU. Both planets are embedded in a 30 $M_\oplus$ disk, extending from 10 to 50 AU with a r^{-1} surface density profile (7.5 $M_\oplus$ between 40 and 50 AU). The pair of black curves show the evolution of Neptune's perihelion and aphelion distance, while the grey curves refer to the embryo. Notice that the embryo is never scattered by Neptune, unlike in Petit et al. simulations. It migrates through the disk faster than Neptune until the disk's outer edge. Neptune interacts with the entire mass of the disk, thanks to the dynamical excitation of the latter due to the presence of the embryo. Therefore, it migrates much further that it would if the embryo were not present, and reaches a final position well beyond 30 AU (it reaches 40 AU after 1 Gy).

resonance sweeping (Nagasawa and Ida, 2000). Therefore, we conclude that Neptune never saw the missing mass of the Kuiper belt. The remaining possibility for a dynamical depletion of the Kuiper belt is that the Kuiper belt objects were kicked directly to hyperbolic or Jupiter-crossing orbit and consequently were eliminated without interacting with Neptune. Only the passage of a star through the Kuiper belt seems to be capable of such an extreme excitation (Kobayashi and Ida, 2001).

The collisional grinding scenario was proposed by Stern and Colwell (1997) and Davis and Farinella (1997, 1998). A massive Kuiper belt with large eccentricities and inclinations would undergo a very intense collisional activity. Consequently, most of the mass originally incorporated in bodies smaller than 50–100 km in size could be comminuted into dust, and then evacuated by radiation pressure and Poynting-Robertson drag. This would cause a substantial mass depletion, provided that the bodies larger than 50 km (which cannot be efficiently destroyed by collisions) initially represented only a small fraction of the total mass.

The collisional grinding scenario, however, has several apparent problems. First, it requires a peculiar size distribution, such that all of the missing mass was contained in small, easy to break, objects, while the number of large object was essentially identical to the current one.

Second, in order to reduce the mass of the Kuiper belt to less than an Earth mass over the age of the Solar System, Stern and Colwell (1997) required a large eccentricity and inclination excitation ($e \sim 0.25$ and/or $i \sim 7°$). This excitation is significantly larger than that characterizing the cold population.

Third, many of the binaries in the cold population would not survive the collisional grinding phase (Petit and Mousis, 2003). In fact, the Kuiper belt binaries have large separations, so that it can be easily computed that the impact on the satellite of a 100 times less massive projectile with a speed of 1km/s would give the former an impulse velocity sufficient to escape to an unbound orbit. If the collisional activity was strong enough to cause an effective reduction of the overall mass of the Kuiper belt these kind of collisions had to be extremely common, so that we would not expect a significant fraction of widely separated binary objects in the current remaining population.

A possible way out of this mass depletion problem has been recently proposed by Levison and Morbidelli (2003). In their preferred scenario, the primordial edge of the massive protoplanetary disk was somewhere around 30–35 AU and the *entire* Kuiper belt population – not only the hot component as in Gomes's scenario – formed within this limit and was transported to its current location during Neptune's migration. The transport process of the cold population was different from the one found by Gomes (2003) for the hot population. These bodies were trapped in the 1:2 resonance with Neptune and transported outwards within the resonance, until they were progressively released due to the non-smoothness of the planetary migration. In the standard adiabatic migration scenario (Malhotra, 1995) there would be a resulting correlation between the eccentricity and the semi-major axis of the released bodies. However this correlation is broken by a secular resonance embedded in the 1:2 mean motion resonance. This secular resonance is generated because the precession rate of Neptune's orbit is modified by the torque exerted by the massive protoplanetary disk that drives the migration. Simulations of this process allow one to match the observed (a, e) distribution of the cold population fairly well (see Figure 10), while the initially small inclinations are only very moderately perturbed. In this scenario, the small mass of the current Kuiper belt population is simply the due to the fact that presumably only a small fraction of the massive disk population was initially trapped in the 1:2 resonance and released on stable non-resonant orbits. The preservation of the binary objects is not a problem because these objects were moved out of the massive disk in which they formed by a gentle dynamical process. The final position of Neptune would simply reflect the primitive truncation of the protoplanetary disk. Conversely, this model opens

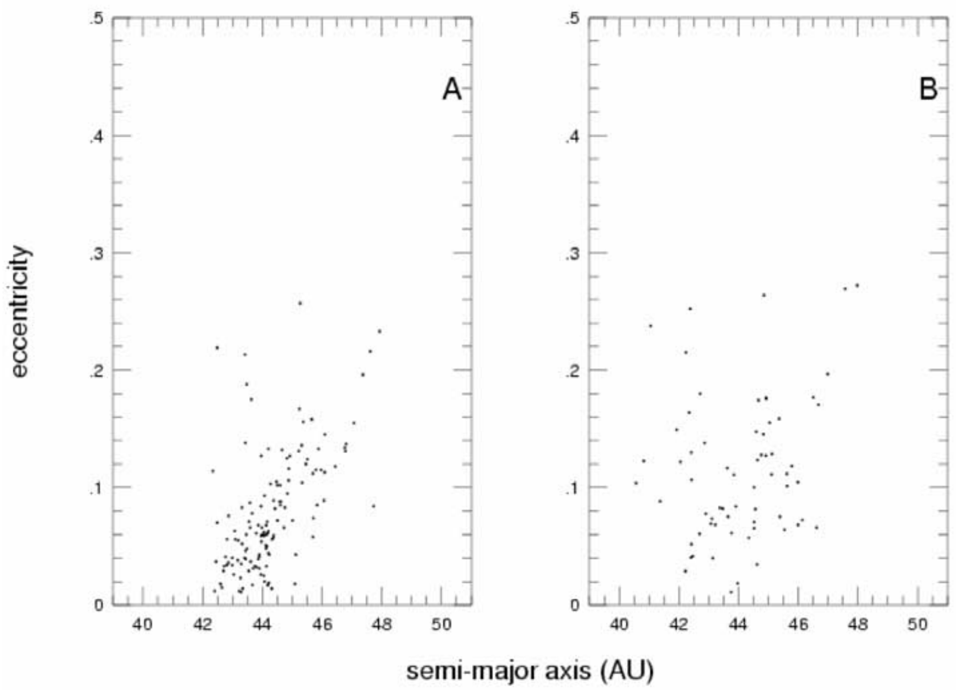

Figure 10. Left: the observed semi-major axis vs eccentricity distribution of the cold population. Only bodies with multi-opposition orbits and $i < 4°$ are taken into account. Right: the resulting orbital distribution in the scenario proposed by Levison and Morbidelli (2003).

again the problem of the origin of different physical properties of the cold and hot populations, because they would have both originated within 35 AU, although in somewhat different parts of the disk. At the time of writing, this innovative model has not yet been critically debated within the community. But this scenario does a simple prediction that will be confirmed or denied by future observations: the edge of the cold classical belt is exactly at the location of the 1:2 resonance.

5. Conclusions and Perspectives

Ten years of dedicated surveys have revealed unexpected and intriguing properties of the trans-Neptunian population, such as the existence of a large number of bodies trapped in mean motion resonances, the overall mass deficit, the large orbital eccentricities and inclinations, the apparent existence of an outer edge at ~ 50 AU and of a correlation among inclinations, sizes and colours. Understanding how the Kuiper belt acquired all these properties would probably constrain several aspects of the formation of the outer planetary system and of its primordial evolution.

Up to now, a portfolio of scenarios have been proposed by theoreticians. None of them can account for all the observations alone, and the solution of the Kuiper belt primordial sculpting problem probably requires a combination of the proposed models. The Malhotra–Gomes scenario on the effects of planetary migration does a quite good job at reproducing the observed orbital distribution inside 50 AU. The apparent edge of the belt at 50 AU might be explained by a very early stellar encounter at $\sim$ 150–200 AU. The origin of the peculiar orbit of 2000 CR_{105} could be due to a later stellar encounter at $\sim$ 800 AU.

The most mysterious feature that remains unexplained in this combination of scenarios is the mass deficit of the cold classical belt. This suggests the possibility, proposed by Levison and Morbidelli (2003) that the primordial planetesimal disk was truncated inside 40 AU and that also the cold population was pushed out from within this edge, during Neptune's migration.

Kuiper belt science is a rapidly evolving one. New observations change our view of the belt every year. Since the discovery of the first trans-Neptunian object 10 years ago several review papers have been written, and all of them are already obsolete. No doubt that this will also be the fate of this chapter, but it can be hoped that the ideas presented here can continue to guide us in the direction of further understanding of what present observations of the Kuiper belt can tell us about the formation and evolution of the outer solar system.

References

Allen, R. L., Bernstein, G. M., and Malhotra, R.: 2001, 'The Edge of the Solar System', *Astroph. J.* **549**, L241–L244.

Allen, R. L., Bernstein, G. M., and Malhotra, R.: 2002, 'Observational Limits on a Distant Cold Kuiper Belt', *Astron. J.* **124**, 2949–2954.

Bate, M. R., Bonnell, I. A., and Bromm, V.: 2003, 'The Formation of a Star Cluster: Predicting the Properties of Stars and Brown Dwarfs', *M.N.R.A.S.* **339**, 577–599.

Brown, M.: 2001, 'The Inclination Distribution of the Kuiper Belt', *Astron. J.* **121**, 2804–2814.

Brown, M. E. and Trujillo, C. A.: 2003, 'The Plane of the Kuiper Belt', in preparation.

Brunini, A. and Melita, M.: 2002, 'The Existence of a Planet Beyond 50 AU and the Orbital Distribution of the Classical Edgeworth Kuiper Belt Objects', *Icarus* **160**, 32–43.

Chiang, E. I. and Brown, M. E.: 1999, 'Keck Pencil-beam Survey for Faint Kuiper Belt Objects', *Astron. J.* **118**, 1411–1422.

Chiang, E. I., Jordan, A. B., Millis, R. L., Buie, M. W., Wasserman, L. H., Elliot, J. L., Kern, S. D., Trilling, D. E., Meech, K. J., and Wagner, R. M.: 2003, 'Resonance Occupation in the Kuiper Belt: Case Examples of the 5:2 and Trojan Resonances', *Astron. J.* **126**, 430–443.

Cohen, C. J. and Hubbard, E. C.: 1965, 'The Orbit of Pluto', *The Observatory* **85**, 43–44.

Davis, D. R. and Farinella, P.: 1997, 'Collisional Evolution of Edgeworth-Kuiper Belt Objects', *Icarus* **125**, 50—60.

Davis, D. R. and Farinella, P.: 1998, 'Collisional Erosion of a Massive Edgeworth-Kuiper Belt: Constraints on the Initial Population', *Lunar Planet. Science Conf.* **29**, 1437–1438.

Dones, L.: 1997, in Y. J. Pendleton & A. G. G. M. Tielens (eds.), *ASP Conf. Ser. 122, From Stardust to Planetesimals*, San Francisco: ASP, 347.

Doressoundiram, A., Barucci, M. A., Romon, J., and Veillet, C.: 2001, 'Multicolor Photometry of Trans-neptunian Objects', *Icarus* **154**, 277–286.

Duncan, M. J., Levison, H. F., and Budd, S. M.: 1995, 'The Long-term Stability of Orbits in the Kuiper Belt', *Astron. J.* **110**, 3073–3083.

Duncan, M. J. and Levison, H. F.: 1997, 'Scattered Comet Disk and the Origin of Jupiter Family Comets', *Science* **276**, 1670–1672.

Fernández, J. A. and Ip, W. H.: 1996, 'Orbital Expansion and Resonant Trapping During the Late Accretion Stages of the Outer Planets', *Pl. Sp. Sci.* **44**, 431–439.

Garcia-Sanchez, J., Weissman, P. R., Preston, R. A., Jones, D. L., Lestrade, J. F., Latham, D. W., Stefanik, R. P., and Paredes, J. M.: 2001, 'Stellar Encounters with the Solar System', *Astron. Astropys.* **379**, 634–659.

Gladman, B., Kavelaars, J. J., Nicholson, P. D., Loredo, T. J., and Burns, J. A.: 1998, 'Pencil-beam Surveys for Faint Trans-Neptunian Objects', *Astron. J.* **116**, 2042–2054.

Gladman, B., Kavelaars, J. J., Petit, J. M., Morbidelli, A., Holman, M. J., and Loredo, Y.: 2001, 'The Structure of the Kuiper Belt: Size Distribution and Radial Extent', *Astron. J.* **122**, 1051–1066.

Gladman, B., Holman, M., Grav, T., Kaavelars, J. J., Nicholson, P., Aksnes, K., and Petit, J. M.: 2002, 'Evidence for an Extended Scattered Disk', *Icarus* **157**, 269–279.

Goldreich, P., Lithwick, Y., and Sari, R.: 2002, 'Formation of Kuiper-belt Binaries by Dynamical Friction and Three-body Encounters', *Nature* **420**, 643–646.

Gomes, R. S.: 2000, 'Planetary Migration and Plutino Orbital Inclinations', *Astron. J.* **120**, 2695–2707.

Gomes, R. S.: 2003, 'The Origin of the Kuiper Belt High Inclination Population', *Icarus* **161**, 404–418.

Gomes, R. S., Morbidelli, A., and Levison, H. F.: 2003, 'Planetary Migration in a Planetesimal Disk: Why Did Neptune Stop at 30 AU?' *Icarus*, in press.

Hahn, J. M. and Malhotra, R.: 1999, 'Orbital Evolution of Planets Embedded in a Planetesimal Disk', *Astron. J.* **117**, 3041–3053.

Hainaut, O.: 2002, http://www.sc.eso.org/ ohainaut/MBOSS/

Henrard, J.: 1982, 'Capture into Resonance – An Extension of the Use of Adiabatic Invariants', *Cel. Mech.* **27**, 3–22.

Ida, S., Larwood, J., and Burkert, A.: 2000, 'Evidence for Early Stellar Encounters in the Orbital Distribution of Edgeworth-Kuiper Belt Objects', *Astroph. J.* **528**, 351–356.

Jewitt, D. C. and Luu, J. X.: 1993, 'Discovery of the Candidate Kuiper Belt Object 1992 QB1', *Nature* **362**, 730–732.

Jewitt, D., Luu, J., and Chen, J.: 1996, 'The Mauna-Kea-Cerro-Totlolo (MKCT) Kuiper Belt and Centaur Survey', *Astron. J.* **112**, 1225–1232.

Jewitt, D., Luu, J., and Trujillo, C.: 1998, 'Large Kuiper Belt Objects: The Mauna Kea 8K CCD Survey', *Astron. J.* **115**, 2125–2135.

Kenyon, S. J. and Luu, J. X.: 1998, 'Accretion in the Early Kuiper Belt: I. Coagulation and Velocity Evolution', *Astron. J.* **115**, 2136–2160.

Kenyon, S. J. and Luu, J. X.: 1999a, 'Accretion in the Early Kuiper Belt: II. Fragmentation', *Astron. J.* **118**, 1101–1119.

Kenyon, S. J. and Luu, J. X.: 1999b, 'Accretion in the Early Outer Solar System', *Astrophys. J.* **526**, 465–470.

Kenyon, S. J. and Bromley, B. C.: 2002, 'Collisional Cascades in Planetesimal Disks. I. Stellar Flybys', *Astron. J.* **2002**, 1757–1775.

Kobayashi, H. and Ida, S.: 2001, 'The Effects of a Stellar Encounter on a Planetesimal Disk', *Icarus* **153**, 416–429.

Kuchner, M. J., Brown, M. E., and Holman, M.: 2002, 'Long-Term Dynamics and the Orbital Inclinations of the Classical Kuiper Belt Objects', *Astron. J.* **124**, 1221–1230.

Kuiper, G. P.: 1951, 'On the Origin of the Solar System', in Hynek, J. A. (ed.), *Astrophysics*, McGraw-Hill, New York, 357 pp.

Levison, H. F. and Duncan, M. J.: 1997, 'From the Kuiper Belt to Jupiter-Family Comets: The Spatial Distribution of Ecliptic Comets', *Icarus* **127**, 13–32.

Levison, H. F. and Stern, S. A.: 2001, 'On the Size Dependence of the Inclination Distribution of the Main Kuiper Belt', *Astron. J.* **121**, 1730–1735.

Levison, H. F. and Morbidelli, A.: 2003, 'Pushing Out the Kuiper Belt', *Nature* **426**, 419–421.

Levison, H. F., Morbidelli, A., and Dones, L.: 2003, 'Forming the Outer Edge of the Kuiper Belt by a Stellar Encounter: Constrints from the Oort Cloud', in preparation.

Lewis, J. S.: 1995, *Physics and Chemistry of the Solar System*, Academic Press, San Diego.

Malhotra, R.: 1993, 'The Origin of Pluto's Peculiar Orbit', *Nature* **365**, 819–821.

Malhotra, R.: 1995, 'The Origin of Pluto's Orbit: Implications for the Solar System Beyond Neptune', *Astron. J.* **110**, 420–432.

Melita, M., Larwood, J., Collander-Brown, S., Fitzsimmons, A., Williams, I. P., and Brunini, A.: 2002, 'The Edge of the Edgeworth-Kuiper Belt: Stellar Encounter, Trans-Plutonian Planet or Outer Limit of the Primordial Solar Nebula?', in *Asteroid, Comet, Meteors*, ESA Spec. Publ. series, 305–308.

Morbidelli, A. and Valsecchi, G. B.: 1997, 'Neptune Scattered Planetesimals Could have Sculpted the Primordial Edgeworth–Kuiper Belt', *Icarus* **128**, 464–468.

Morbidelli, A. and Brown, M.: 2003, 'The Kuiper Belt and the Primordial Evolution of the Solar System', in Festou et al. (eds.), *Comet II*, University Arizona Press, Tucson, AZ, in press.

Morbidelli, A. and Levison, H. F.: 2003, 'Scenarios for the Origin of the Trans-Neptunian Object 2000 CR_{105}', in preparation.

Nagasawa, M. and Ida, S.: 2000, 'Sweeping Secular Resonances in the Kuiper Belt Caused by Depletion of the Solar Nebula', *Astron. J.* **120**, 3311–3322.

Petit, J. M., Morbidelli, A., and Valsecchi, G. B.: 1999, 'Large Scattered Planetesimals and the Excitation of the Small Body Belts', *Icarus* **141**, 367–387.

Petit, J. M. and Mousis, O.: 2003, 'KBO Binaries: Are They Really Primordial?', *Icarus*, submitted.

Stern, S. A.: 1995, 'Collisional Time Scales in the Kuiper Disk and Their Implications', *Astron. J.* **110**, 856–868.

Stern, S. A.: 1996, 'On the Collisional Environment, Accretion Time Scales, and Architecture of the Massive, Primordial Kuiper Belt', *Astron. J.* **112**, 1203–1210.

Stern, S. A. and Colwell, J. E.: 1997a, 'Accretion in the Edgeworth-Kuiper Belt: Forming 100–1000 KM Radius Bodies at 30 AU and Beyond', *Astron. J.* **114**, 841–849.

Stern, S. A. and Colwell, J. E.: 1997b, 'Collisional Erosion in the Primordial Edgeworth-Kuiper Belt and the Generation of the 30–50 AU Kuiper Gap', *Astroph. J.* **490**, 879–885.

Stern, S. A.: 2002, 'Evidence for a Collisonal Mechanism Affecting Kuiper Belt Object Colors', *Astron. J.* **124**, 2297–2299.

Tegler, S. C. and Romanishin, W.: 2000, 'Extremely Red Kuiper-belt Objects in Near-circular Orbits Beyond 40 AU', *Nature* **407**, 979–981.

Thebault, P. and Doeressoundiram, A.: 2003, 'A Numerical Test of the Collisional Resurfacing Scenario. Could Collisional Activity Explain the Spatial Distribution of Color-index Within the Kuiper Belt?', *Icarus* **162**, 27–37.

Trujillo, C. A. and Brown, M. E.: 2001, 'The Radial Distribution of the Kuiper Belt', *Astroph. J*. **554**, 95–98.

Trujillo, C. A., Jewitt, D. C., and Luu, J. X.: 2001, 'Properties of the Trans-Neptunian Belt: Statistics from the Canada-France-Hawaii Telescope Survey', *Astron. J.* **122**, 457–473.

Trujillo, C. A. and Brown, M. E.: 2002, 'A Correlation between Inclination and Color in the Classical Kuiper Belt', *Astroph. J*. **566**, 125–128.

Trujillo, C. A. and Brown, M. E.: 2003, 'The Caltech Wide Area Sky Survey: Beyond (50000) Quaoar', submitted to *Proceedings of the First Decadal Review of the Edgeworth-Kuiper Belt Meeting in Antofagasta*, Chile, to be published in *Earth Moon and Planets*.
Weidenschilling, S.: 2002, 'On the Origin of Binary Transneptunian Objects', *Icarus* **160**, 212–215.
Weidenschilling, S.: 2003, 'Formation of Planetesimals/Cometesimals in the Solar nebula', in Festou et al. (eds.), *Comet II*, University Arizona Press, Tucson, AZ.